Mesoscale Iron Enrichment Experiments 1993–2005: Synthesis and Future Directions

P. W. Boyd,[1]* T. Jickells,[2] C. S. Law,[3] S. Blain,[4] E. A. Boyle,[5] K. O. Buesseler,[6] K. H. Coale,[7] J. J. Cullen,[8] H. J. W. de Baar,[9] M. Follows,[5] M. Harvey,[3] C. Lancelot,[10] M. Levasseur,[11] N. P. J. Owens,[12] R. Pollard,[13] R. B. Rivkin,[14] J. Sarmiento,[15] V. Schoemann,[10] V. Smetacek,[16] S. Takeda,[17] A. Tsuda,[18] S. Turner,[2] A. J. Watson[2]

Since the mid-1980s, our understanding of nutrient limitation of oceanic primary production has radically changed. Mesoscale iron addition experiments (FeAXs) have unequivocally shown that iron supply limits production in one-third of the world ocean, where surface macronutrient concentrations are perennially high. The findings of these 12 FeAXs also reveal that iron supply exerts controls on the dynamics of plankton blooms, which in turn affect the biogeochemical cycles of carbon, nitrogen, silicon, and sulfur and ultimately influence the Earth climate system. However, extrapolation of the key results of FeAXs to regional and seasonal scales in some cases is limited because of differing modes of iron supply in FeAXs and in the modern and paleo-oceans. New research directions include quantification of the coupling of oceanic iron and carbon biogeochemistry.

The work of John Martin (1, 2) sharply focused attention on the role of iron (Fe) in ocean productivity, biogeochemical cycles, and global climate by proposing "that phytoplankton growth in major nutrient-rich waters is limited by iron deficiency" (2). The candidate mechanism of Martin (1, 2) points to the importance of changes, over geological

[1]National Institute for Water and Atmospheric Research (NIWA) Centre for Chemical and Physical Oceanography, Department of Chemistry, University of Otago, Dunedin, New Zealand. [2]School of Environmental Sciences, University of East Anglia, Norwich NR4 7TJ, UK. [3]NIWA, Evans Bay Parade, Kilbirnie, Wellington, New Zealand. [4]Laboratoire d'Océanographie et de Biogéochimie, Campus de Luminy, Case 901, F-16288 Marseille Cedex 09, France. [5]Department of Earth, Atmosphere and Planetary Sciences, Massachusetts Institute of Technology, Cambridge, MA 02139, USA. [6]Marine Chemistry and Geochemistry, Woods Hole Oceanographic Institution, Woods Hole, MA 02543, USA. [7]Moss Landing Marine Laboratories, 8272 Moss Landing Road, Moss Landing, CA 95039, USA. [8]Department of Oceanography, Dalhousie University, Halifax, Nova Scotia B3H 4J1, Canada. [9]Royal Netherlands Institute for Sea Research, 1790 AB Den Burg, Netherlands. [10]Ecologie des Systèmes Aquatiques, Université Libre de Bruxelles, B-1050 Bruxelles, Belgium. [11]Département de Biologie (Québec-Océan), Université Laval, Ste-Foy, Québec G1K 7P4, Canada. [12]Plymouth Marine Laboratory, Prospect Place, The Hoe, Plymouth PL1 3DH, UK. [13]National Oceanography Centre, Southampton, University of Southampton, Southampton SO14 3ZH, UK. [14]Ocean Sciences Centre, Memorial University of Newfoundland, St. John's, Newfoundland A1C 5S7, Canada. [15]Atmospheric and Oceanic Sciences Program, Princeton University, Sayre Hall, Forrestal Campus, Princeton, NJ 08544, USA. [16]Alfred Wegener Institute for Polar and Marine Research, 27570 Bremerhaven, Germany. [17]Graduate School of Agricultural and Life Sciences, University of Tokyo, Yayoi 1-1-1, Bunkyo-ku, Tokyo 113-8657, Japan. [18]Ocean Research Institute, University of Tokyo, Tokyo 113-8657, Japan.

*To whom correspondence should be addressed. E-mail: pboyd@alkali.otago.ac.nz

time, in the magnitude of macronutrient uptake by phytoplankton in waters where macronutrient concentrations are perennially high (1). Specifically, Fe supply to the ocean was much higher during glacial maxima than at present (1), and it is estimated that the increase in Fe-induced productivity could have contributed perhaps 30% of the 80-ppm drawdown in atmospheric CO_2 observed during glacial maxima by enhancing the ocean's biological pump (3).

Early results from shipboard incubations in high nutrient–low chlorophyll (HNLC) waters presented compelling but equivocal evidence that phytoplankton growth was limited by Fe availability (2). After rigorous discussion, a consensus was reached (4) that, because shipboard experiments have artifacts, mesoscale Fe addition experiments (FeAXs) offered the best approach to resolve questions about the role of Fe in ocean productivity, C cycling, and climate. The main objective of FeAXs was to test whether Fe enrichment would increase primary productivity in HNLC waters, but additional questions focused on how Fe enrichment would affect nutrient use and export (1).

The era of mesoscale Fe enrichments started with IronEx I, where Fe and the conservative tracer SF_6 (5) were added to tropical HNLC surface waters (6). A further 11 FeAXs of similar design (7, 8) in different HNLC regions (Fig. 1) later confirmed the capability to study pelagic ecology and biogeochemical cycling in a discrete water parcel over time and space scales of weeks and kilometers. Complementary approaches include ship-based observations of persistent blooms within HNLC waters (Fig. 1),

termed here FeNXs (Fe natural enrichment experiments), that are driven by sustained and localized Fe enrichment (9).

Common Findings in FeAXs

FeAXs have each used a common framework (7) that enables comparison of their biogeochemical signatures (Table 1 and tables S1 to S3). The results of FeAXs have substantially increased our understanding of ecological and biogeochemical dynamics and their interrelationships, and many findings are consistent with theory-based predictions of ecosystem dynamics. For example, they have shown that phytoplankton grow faster in warmer open-ocean waters (table S2), as predicted by algal physiological relationships (10), and that blooms across a range of FeAX sites display an inverse relationship between chlorophyll concentration and mixed-layer depth (Table 1), as forecast by theoretical relationships between light penetration and mixed-layer depth (8, 11, 12). More specifically, FeAXs have verified that Fe enrichment enhances primary production from polar to tropical HNLC waters (Table 1) and confirmed that Fe supply has a fundamental role in photosynthesis (photosynthetic competence, table S1), diatom sinking, Fe uptake rates (13), and other physiological processes. FeAXs have demonstrated reduced silica requirements of diatoms when relieved of Fe stress (14), confirming results from bottle experiments (15).

These mesoscale experiments have provided detailed time-series observations, within a tracer-labeled parcel of water [i.e., a Lagrangian framework (7)], of open-ocean blooms from initiation through evolution and decline (Table 1). Data collection within a Lagrangian framework gives unparalleled insights into bloom dynamics and clarifies how the interplay of factors such as initial conditions (table S1) and loss processes defines properties such as bloom magnitude, which exhibits a factor of 10 range in chlorophyll concentrations between FeAXs (Table 1). The broad suite of measurements and their high temporal resolution in FeAXs will be a useful tool to better interpret the less highly resolved observations available for naturally occurring blooms [e.g., the Antarctic Environment and Southern Ocean Process Study (AESOPS) (16)]. Furthermore, the high-resolution data sets have enabled the establishment of a mechanistic understanding, in some FeAXs, of the evolution, termination, and decline phases of blooms (17) (Table 1). The durations of these bloom phases provide an estimate of the lag time between the accumulation of phytoplankton C and its subsequent export (17); such an estimate has proved elusive in previous studies (18).

This experimental approach has presented a platform to examine in detail the interactions of top-down and bottom-up control—outlined in the ecumenical Fe hypothesis (19)—on phy-

toplankton community structure. For example, stocks of all phytoplankton groups increased initially upon Fe enrichment, but only the diatoms bloomed (Table 1) by escaping grazing pressure. Thus, unlike bottle incubations, FeAXs offer a holistic approach to studying the entire pelagic food web. This enables assessment of the interplay of ecological processes and the resultant biogeochemical signals, such as Fe-mediated increases in haptophyte abundances (table S2) and consequent faunistic shifts within the microzooplankton (20) (table S2) that lead to changes in dimethyl sulfoniopropionate (DMSP) (20) and dimethyl sulfide (DMS) concentrations (20) (Table 1), respectively. These changes in DMS concentration demonstrate that climate-reactive biogenic gases—in addition to CO_2—must be considered to obtain the cumulative effect of Fe enrichment on climate.

The scale of FeAXs, and in particular their use of the SF_6 tracer, enabled the construction of pelagic biogeochemical budgets for C (17) and Fe (21) under high-Fe conditions. FeAXs have permitted the study of whether speciation controls Fe bioavailability (22), the mechanisms behind changes in the production of Fe-binding ligands (FeBLs) in response to enhanced Fe (table S3), and other aspects of Fe chemistry. The SF_6 tracer has also helped demonstrate that the underlying physics at FeAX sites alters the bloom biogeochemical signature both by diluting phytoplankton stocks (Table 1) and by increasing the macronutrient inventory of the patch (table S3). Such patch dilution may result in experimental artifacts including arrested bloom development (23), which leads to reduced macronutrient uptake.

Together, the wide range of experimental conditions and resulting breadth of bloom signatures evident from FeAXs (Table 1 and tables S1 to S3) provide an essential data resource to improve existing ecological and biogeochemical models and to develop new ones. For example, a new model of DMS dynamics developed during Subarctic Ecosystem Response to Iron Enrichment Study (SERIES) provides a better understanding of how the complex interplay of physical, photochemical, and biological processes affects the temporal evolution of mixed-layer DMS concentrations (24).

Scaling Up the Results from FeAXs

A key issue to be addressed is how natural or anthropogenic variability in Fe supply affects
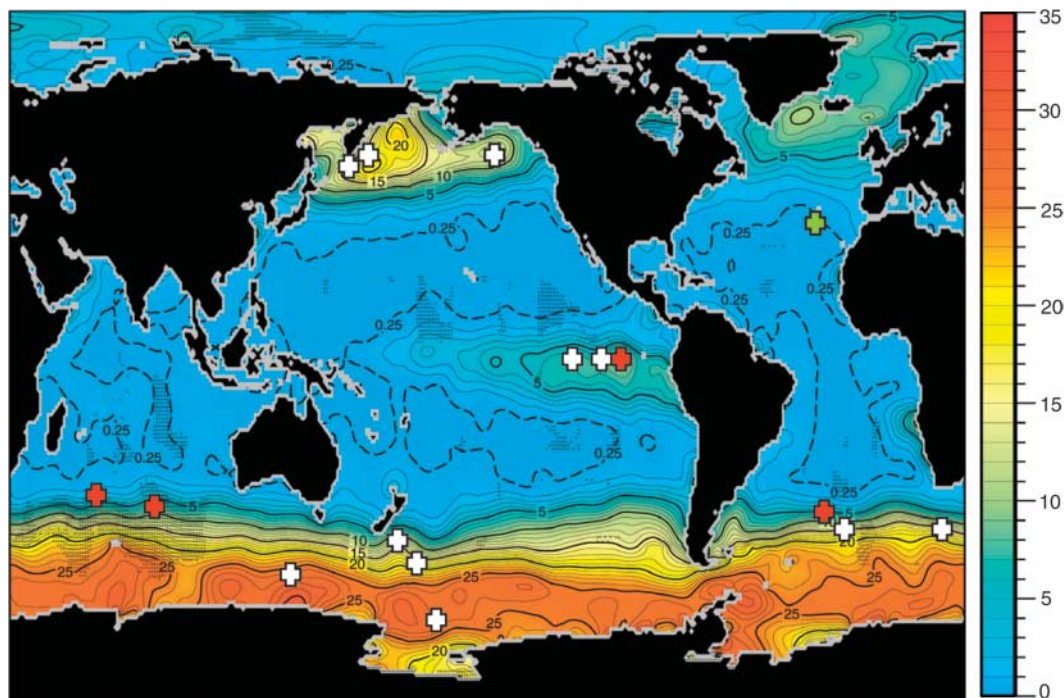

Fig. 1. Annual surface mixed-layer nitrate concentrations in units of μmol liter^{-1} (48), with approximate site locations of FeAXs (white crosses), FeNXs (red crosses), and a joint Fe and P enrichment study of the subtropical LNLC Atlantic Ocean (FeeP; green cross). FeAXs shown are SEEDS I and II (northwest Pacific; same site but symbols are offset), SERIES (northeast Pacific), IronEX I and II (equatorial Pacific; IronEX II is to the left), EisenEx and EIFEX (Atlantic polar waters; EIFEX is directly south of Africa), SOIREE (polar waters south of Australia), SOFEX-S (polar waters south of New Zealand), SOFEX-N (subpolar waters south of New Zealand), and SAGE (subpolar waters nearest to New Zealand). FeNX sites shown are the Galapagos Plume (equatorial Pacific), Antarctic Polar Front (polar Atlantic waters), and the Crozet and Kerguelen plateaus (Indian sector of Southern Ocean; Crozet is to the left of Kerguelen). For the geographical positions of the FeAXs, see (8). FeeP investigated whether N-fixing phytoplankton are simultaneously limited by Fe and P; see Table 1.

ocean biogeochemistry and global climate (25). FeAXs are relatively short-term experiments specifically designed to test whether Fe supply limits primary production in HNLC waters, and therefore they can address this issue only by extrapolation. Here, we consider whether findings from FeAXs can successfully be scaled up temporally (seasonal to geological) and spatially (regional to global). Four issues, addressed below, are central to tests of the validity of such extrapolation.

Macronutrient Uptake

The degree of Fe-mediated algal uptake of the mixed-layer macronutrient inventory will determine bloom longevity (17) and influence the magnitude of C sequestration (1, 3). FeAXs, on a time scale of weeks, have exhibited a wide range of nutrient uptake (table S3), with depletion of >0.75 and >0.6 of the mixed-layer silicate and nitrate inventory, respectively, in several cases (table S2). Polar FeAXs, although of longer duration (Table 1), have resulted in <0.3 of the macronutrient inventory being used, although inventories at polar FeAX sites are greater than in other HNLC regions (table S2). Fe-mediated diatom blooms in both FeAXs (table S2) and natural conditions (16, 26) can deplete silicate but not nitrate, which has led to

bloom decline. SERIES suggests that both Fe supply and diatom species succession, as a result of decreasing silicate concentrations, set the silicate:nitrate uptake stoichiometry (17). Thus, although longer-term Fe enrichment (months) may result in uptake of a greater proportion of the macronutrient inventory, it is difficult to scale up the findings of FeAXs without information on the long-term stability of phytoplankton community structure, such as diatom species succession (17).

Mediation of bloom decline via macronutrient depletion means that grazer control of phytoplankton stocks is less likely on the shorter time scales typical of FeAXs. This may also apply in some cases to the Last Glacial Maximum, as abundant diatom resting spores from Southern Ocean sediment cores indicate substantial export from diatom blooms in the Atlantic sector triggered by nutrient exhaustion rather than grazer control (27). Thus, FeAXs may mimic naturally occurring blooms that are transient (weeks) and are terminated by rapid nutrient depletion with consequently little change in the grazer community (17).

Bloom Time Scales and Food Web Dynamics

FeAX blooms may be subject to zooplankton grazing (Table 1), which would result in less

efficient downward export of algal C (20) and an increase in pelagic Fe recycling (28). However, the generation times for grazers range from days (microzooplankton) to months (macrozooplankton), whereas FeAX blooms evolve over 2 to 3 weeks (Table 1). Increased microzooplankton and, in some cases, mesozooplankton abundances (Table 1 and table S2) and subsequent alteration of food web dynamics were evident during FeAX blooms (table S2). If FeAXs were of longer duration, would stocks of large zooplankton increase with sustained Fe-elevated productivity? If so, how would they influence the bloom signature? Heavy grazing pressure, exerted by macrozooplankton, occurs in some upwelling regions (29) where a continuous nutrient supply (months) maintains a high-productivity system. Recent FeNXs, at sites with sustained

nutrient supply (9), will reveal whether such an adaptive grazer response occurs during long-term blooms within HNLC waters, and hence whether upscaling the results of FeAXs to sustained naturally occurring blooms (months) is valid. If such an adaptive grazer response is observed, the potential long-term biogeochemical feedbacks of grazer-mediated Fe recycling and reduced export efficiency of algal C should be explored via modeling simulations.

Modes of Iron Supply

Initial attempts to relate the Fe supply during FeAXs with that in the modern or paleo-ocean (30) were hampered by relatively poor understanding of Fe biogeochemistry. Since the mid-1990s, our understanding has advanced considerably through better estimates of the solubility (31) and upper ocean residence time

of aerosol Fe (32), improved regional coverage of dissolved Fe (DFe) concentrations (33), and greater insight into the key role of FeBL in maintaining Fe in the upper ocean (34). Although measuring DFe remains challenging, many technical issues have now been addressed (35). Our improved understanding is reflected in better models of dust depositional fluxes (25), oceanic DFe distributions (36), and the impact of higher Fe supply to the paleo-ocean (14), providing a more realistic picture of Fe supply to HNLC waters both now and in the geological past (Fig. 2).

A comparison of modes of Fe supply in FeAXs, FeNXs, and naturally occurring perturbations (Fig. 2) reveals a wide range in the magnitude, chemistry, residence time, and spatial and temporal scales of Fe supply. Although the pulsed Fe enrichments during FeAXs are

Table 1. The main findings from the 12 FeAXs (in chronological order from left to right) conducted between 1993 and 2005 [for additional details, see (8)]. See tables S1 to S3 for further details of initial conditions, ecosystem structure, and biogeochemical responses. Light climate, defined as the mean irradiance available to phytoplankton in the mixed layer, was calculated according to $I = I_0[1 - \exp(-K_e z)]/K_e z$, where I is mean mixed-layer irradiance (PAR), I_0 is the subsurface PAR, K_e is the vertical light attenuation coefficient (m^{-1}), and z is the depth of the upper mixed layer. Dilution rate is the mean growth rate of the SF$_6$-labeled patch over the duration of each FeAX. Each property is expressed volumetrically but can readily be converted to a column integral by using the data on mixed-layer depth (MLD). Terms prefixed with a delta such as ΔDIC denote maximum minus initial concentrations; nc, no significant change (relative to the surrounding HNLC waters); blank cells indicate that no data are currently available. The ratio of maximum to minimum primary production is based on column integrals.

Property	IronEX I (6)	IronEX II (30)	SOIREE (49)	EisenEx (56)	SEEDS I (57)	SOFEX-S (54, 58)	SOFEX-N (58)	EIFEX (46)	SERIES (17)	SEEDS II (59)	SAGE (59)	FeeP (59)
Fe added (kg)	450	450	1750	2350	350	1300	1700	2820	490	480	1100	1840
Temperature (°C)	23	25	2	3 to 4	11	−1	5	4 to 5	13	9 to 12	11.8	21
Season	Fall	Summer	Summer	Spring	Summer	Summer	Summer	Summer	Summer	Summer	Fall	Spring
Light climate (μmol quanta m^{-2} s^{-1})	254 (max) to 230 (min)	216 to 108	59 to 33	82 to 40	178 to 39	103 to 62	125 to 74		173 to 73		59 to 52	
Dilution rate (day^{-1})	0.27	0.18	0.07	0.04 to 0.43	0.05	0.08	0.1		0.07 to 0.16			0.4
Chlorophyll, $t = 0$ (mg m^{-3})	0.2	0.2	0.2	0.5	0.9	0.2	0.3	0.6	0.4	0.8	0.6	0.04
Chlorophyll, maximum (mg m^{-3})	0.6	3.3	2.3	2.8	23.0	2.5	2.4	3.0	5.5	2.4	1.3	0.07
MLD (m)	35	40*	65*	80*	13	35	45	100	30*	30	70*	30*
Bloom phase (duration, days)	Evolving (5) subducted	Decline (17)	Evolving (13)	Evolving (21)	Evolving (10)	Evolving (28)	Evolving (27)	Partial decline, evolving (37)	Decline (25)	Evolving (25)	No bloom (17)	No bloom (7)
δDIC (mmol m^{-3})	6	26	17	14	58	21	13		36		nc	<1
δDMS (μmol m^{-3})	0.8	1.8	2.9	1.3, then to 0†	nc	nc	Increased		8.5, then to −5.7†	nc	nc	nc
Dominant phytoplankton	Mixed	Diatom	Diatom	Diatom	Diatom	Diatom	Mixed	Diatom	Diatom	Mixed	Mixed	Cyanobacteria Prochlorococcus
Export	nc	increase	nc	nc	nc	Increase	Increase§	Increase	Increase	nc	nc	
Mesozooplankton stocks	Increase‡	Increase	nc	nc	nc	nc	nc	Increase	Increase	Increase	nc	nc
Primary production (max/min ratio)	4	6	9	4	4	6	10	2	10		2	1.7

*Changes in MLD were observed during the study; the maximum MLD is shown (for initial MLD, see table S1). †An initial increase in DMS concentration followed by a decline by the end of the study. ‡Based on anecdotal evidence. §Increased export was mainly associated with a subduction event.
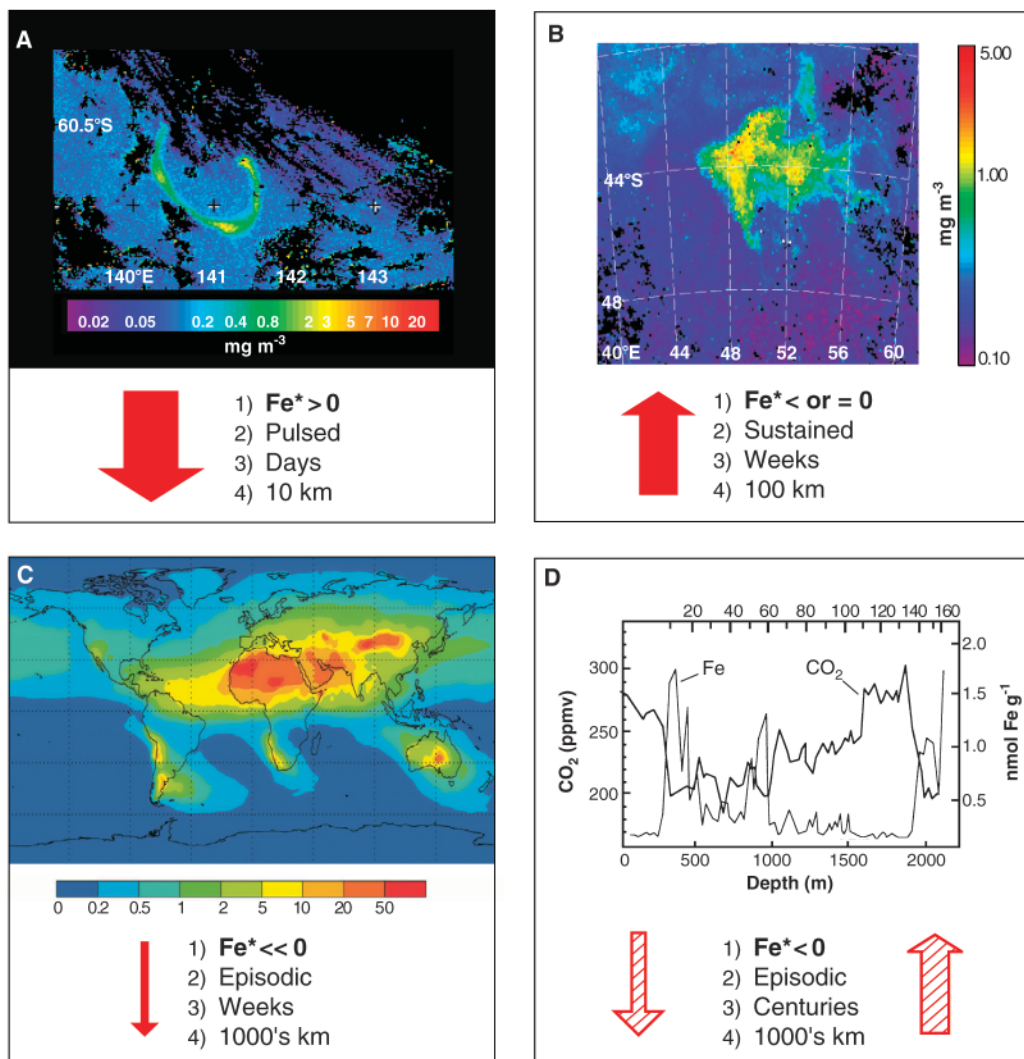
Fig. 2. A comparison for Southern Ocean waters of mechanisms responsible for perturbations in Fe supply. Numbers in each panel: 1) Fe*, the relative magnitude of Fe supply relative to macronutrient supply (36); 2) the mode of Fe supply; 3) the time scale over which surface waters receive increased Fe supply; and 4) the length scales of Fe supply events. (**A**) Satellite image of a purposeful in situ Southern Ocean FeAX [SOIREE (49)]. (**B**) An FeNX near Crozet within the HNLC Southern Ocean, where naturally occurring blooms are evident from remote sensing (9). (**C**) An atmospheric dust deposition event (dust units are g m^{-2} year^{-1}) in the modern Southern Ocean [e.g., from Patagonia (25)]. (**D**) Fe supply to the Southern Ocean during the glacial maxima from direct [i.e., higher dust deposition (1, 39)] and/or indirect [i.e., upwelling of waters with higher Fe concentrations (40)] sources. The magnitude of this supply is unknown; hence, Fe* is expressed as < 0. Fe* is defined as Fe* = [Fe] − {(Fe/P) algal uptake ratio × [PO$_4^{3-}$]} (36). If Fe* > 0, primary production is ultimately macronutrient-limited; if Fe* < 0, production is ultimately Fe-limited. The width of red arrows denotes the relative magnitude of changes in Fe supply; the hatched arrows in (D) denote uncertainties about whether Fe supply in the geological past was episodic or sustained (see text). In (B) to (D), downward- and upward-pointing arrows represent atmospheric and oceanic (upwelling) supply, respectively. Consideration of Fe chemistry for each of these modes of supply is beyond the scope of this review, but see (22).

analogous to episodic dust events, the total Fe supplied in FeAXs is much larger, and Fe solubility is greater than from dust deposition [(7); see also (31)]. Also, there is little evidence of blooms (i.e., >1 mg chlorophyll m^{-3}) after episodic dust deposition into both HNLC (37) and low nutrient–low chlorophyll (LNLC) waters (38).

During the glacial maxima, increases in Fe supply are evident over a time scale of centuries (1). Aerosol Fe supply to the Southern Ocean

during the glacial maxima was higher than at present by a factor of 10 (1, 39). The magnitude of this supply is potentially comparable to that during FeAXs and FeNXs (Fig. 2). However, there are uncertainties about the mode of Fe supply during glacial maxima. Supply was either episodic and localized from dust storms [e.g., Patagonia (39)] and/or sustained and global, being driven by Southern Ocean upwelling and oceanic circulation (40) in conjunction with global dust deposition as the main Fe

source (14). A major unknown in the geological past is the fate of Fe incorporated into phytoplankton blooms. Was dust-mediated Fe supply lost to the deep ocean as declining blooms sank [as aggregates (23)], or was it efficiently recycled by biota in the subsurface ocean and subsequently upwelled? Uncertainty over the fate of Fe is highlighted by comparing two modeling studies. They indicate that substantial atmospheric CO$_2$ drawdown resulted from the routes of high dust deposition with no Fe recycling (41) and from lower rates of dust deposition with recycling and subsequent upwelling (14). The pulsed Fe supply in FeAXs may therefore be more relevant to a paleo-ocean with episodic dust supply (weeks) and Fe export to the deep ocean, whereas FeNXs are a better proxy if Fe supply was sustained (months) by upwelling and recycling. Comparison of the results of FeAXs and FeNXs via modeling studies will provide insights into how different modes of Fe supply affect oceanic Fe and C biogeochemistry.

Coupled Iron-Carbon Biogeochemistry

The degree to which the biogeochemical Fe and C cycles are linked is central to determining the impact of increased Fe supply on atmospheric CO$_2$ drawdown and global climate in the geological past. A key parameter is the efficiency of phytoplankton C fixation per unit DFe [i.e., δ(POC formation)/δ(Fe supplied), where POC is particulate organic carbon], as the resulting δPOC export term will set the atmospheric drawdown efficiency [δ(air-sea CO$_2$ exchange)/δ(POC exported)]. Also, because Fe supply during the geological past was elevated for centuries (Fig. 2D), it is important to determine the fate of C relative to Fe in the upper ocean over longer time scales: Is Fe retained via remineralization in the water column or exported to the sediments? [i.e., δ(DIC remineralized)/δ(Fe remineralized) and δ(POC exported)/δ(PFe exported), where DIC is dissolved inorganic carbon].

There are few published data on Fe/C ratios for particle production, remineralization, or export (Fig. 3). A range of three orders of magnitude in Fe/C molar ratios is evident, which is probably due to the use of different approaches as well as actual differences in C and Fe biogeochemistry. This variability in Fe/C ratios has been

ascribed to a number of processes, such as differential remineralization of Fe and C on sinking particles [due to processes including scavenging on Fe (36, 42)], which results in increased PFe/POC ratios with depth (Fig. 3). Also, phytoplankton in high-Fe surface waters may take up more Fe per unit of C fixed [i.e., "luxury" Fe

paleo-ocean. Key questions center around the issues of macronutrient use, ecosystem responses, modes of Fe supply, and coupling of Fe-C biogeochemical cycles, for which we propose three hypotheses.

First, with respect to macronutrient uptake and ecosystem dynamics, we hypothesize that in

relative importance of the processes that set particulate Fe/C ratios and their controlling factors will vary both regionally and seasonally. These processes, which will dictate Fe and C export, include algal Fe uptake and the differential rates of particle remineralization for Fe and C in surface and subsurface waters. Each
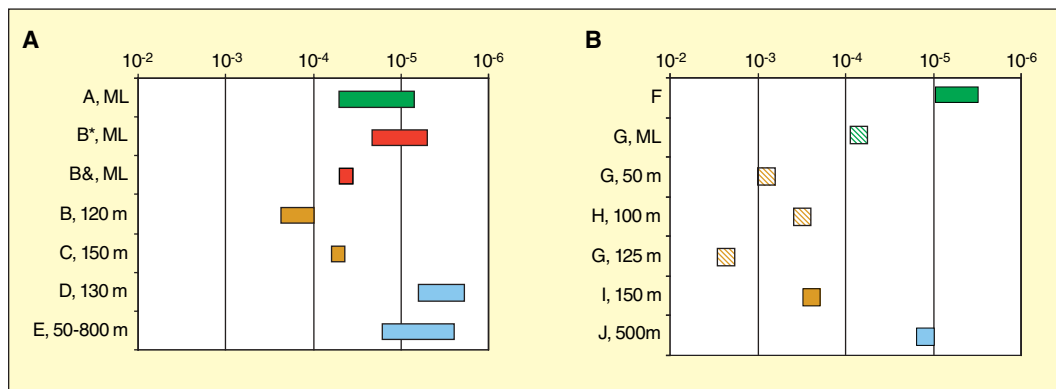

Fig. 3. Summary of published Fe/C molar ratios (on a log scale) from (**A**) low-Fe HNLC waters and (**B**) high-Fe waters and FeAXs (FeAXs denoted by hatched bars). Ratios were obtained from a range of sources: mixed-layer phytoplankton (green), suspended biogenic particles (red), sinking biogenic particles (brown), and remineralization of particles inferred from dissolved constituents (blue). Symbols in (A): A, Southern Ocean (50); B, subantarctic (42); C, subarctic Pacific (51, 52); D, northeast Pacific (1); E, the low-Fe North Atlantic (43); ML, surface mixed-layer samples; *, biogenic Fe only; &, lithogenic and biogenic Fe. Symbols in (B): F, a ratio from an Fe-replete algal culture (53); G, SERIES (17); H, SOFEX-S (54); I, the northeast Atlantic (51); J, the high-Fe North Atlantic (33). The ratios were derived from a wide range of approaches including algal lab cultures (53), sediment traps (42), vertical nutrient profiles in HNLC waters (1), and particle regeneration from apparent oxygen use versus DFe (33, 43). Assessing the bioavailability of Fe (22) is a confounding factor in estimating Fe:C ratios, over and above the effect of patch dilution in FeAXs on the fate of the added Fe. The Fe/C ratios derived from FeAXs in (B) are (Fe added):(C exported) and assume that the Fe term is the total amount of Fe added, which may overestimate this ratio by 100% or more (21, 55).

of these, in turn, will be determined by a range of factors such as DFe concentration [algal Fe uptake (43)], food web structure and grazing activity [remineralization rates (45)], and particle properties and transformations including sinking rate or scavenging [export efficiency (36, 42)].

Testing these hypotheses will require both specific and multistranded approaches that link FeAXs, FeNXs, and biogeochemical Fe and C studies in a range of locales. Three are advocated:

1) Modeling studies to apply our improved understanding of Fe biogeochemistry in the modern ocean to the geological past. Model simulations should also capitalize on the complementary approaches offered by FeAXs and FeNXs into how pulsed versus sustained Fe supply affects ecosystem dynamics and biogeochemistry.

2) Improved experimental designs to overcome the limitations of FeAXs, such as smaller and more frequent Fe doses, greater patch length scale (>>10 km), and additional measurements that provide insight into the impact of Fe enrichment on climate (e.g., biogenic gases) or Fe cycling (e.g., fate of Fe). Detailed comparison of the biogeochemistry of differing FeNXs would help us understand better the influence of a range of Fe:macronutrient stoichiometries on bloom dynamics and C biogeochemistry. Such experiments require application of both existing [aircraft, laser imaging detection and ranging (46)] and new [gliders, sensor arrays (47)] technologies, and should be linked to regional circulation models with embedded biogeochemistry. The utility of shipboard Fe enrichments to study algal physiology in detail should not be overlooked (15).

3) Biogeochemical studies to jointly measure key properties in the Fe and C cycles, such as Fe/C ratios and FeBL concentrations associated with particle transformations, will require specific investigation of end members—HNLC, LNLC, and high-Fe waters in coastal and offshore waters. These, in conjunction with the improved experimental designs described above, will provide insights into temporal and spatial controls on Fe/C ratios in both high- and low-Fe regimes.

uptake (13, 43)], resulting in greater Fe remineralization than C remineralization on sinking particles relative to particles in HNLC waters (33). The available data on PFe/POC ratios indicate that settling particles from natural blooms (northeast Atlantic; Fe/C molar ratio 2.7×10^{-4}) and FeAXs (Fe/C molar ratio 3.1×10^{-4} to 2.1×10^{-3}) have higher ratios than those in HNLC waters (Fig. 3). During FeAXs, much of the Fe added is rapidly lost via precipitation and patch dilution (21); hence, Fe/C ratios from FeAXs will be overestimated by a factor of more than 2 (Fig. 3). Moreover, the time scales of FeAXs do not permit the fate of Fe (recycled or exported) initially added to the mixed layer to be assessed (44), and hence the ultimate efficiency of (Fe added):(C sequestered to depth) cannot be determined. Thus, upscaling the Fe:C stoichiometry from FeAXs to greater spatial and temporal scales is not currently recommended.

The Future: Key Questions and Approaches

Key findings from FeAXs offer insights for modelers, although a limited number of these findings can be extrapolated directly to regional and seasonal scales for Fe enrichment. Such limited extrapolation relates to limitations in the FeAX design (7) and to uncertainties in our understanding of Fe biogeochemistry in the

addition to magnitude, the stoichiometry of macronutrient and Fe supply to HNLC surface waters is equally critical in determining whether blooms are transient (weeks) or sustained (months). This in turn will dictate the planktonic community that develops and the subsequent biogeochemical balance between Fe recycling within, and export from, the surface mixed layer.

Second, although the mode of Fe supply is important (Fig. 2), the factors that influence the availability of the Fe supplied to the biota are critical. We hypothesize that the magnitude of the Fe available to the biota will be determined by the mode of Fe supply and in particular by the subsequent mobilization and retention of this Fe by upper-ocean processes. For aeolian Fe supply, these processes include aerosol Fe mixed-layer residence time (32), photochemistry, FeBL concentrations (25) and their joint impact on aerosol dissolution, and the ability of bacteria to access lithogenic PFe (42). The bioavailability of Fe supplied from upwelling may be influenced by processes such as photochemistry or by the concentration and binding strength of the upwelled Fe and FeBL relative to those in the surface mixed layer.

Regarding the issue of Fe and C biogeochemistry, we offer a third hypothesis: that the

References and Notes

1. J. H. Martin, *Paleoceanography* **5**, 1 (1990).
2. J. H. Martin, R. M. Gordon, S. E. Fitzwater, *Limnol. Oceanogr.* **36**, 1793 (1991).
3. D. M. Sigman, E. A. Boyle, *Nature* **407**, 859 (2000).
4. S. W. Chisholm, F. M. M. Morel, *Limnol. Oceanogr.* **36**, 1507 (1991).
5. A. Watson, P. Liss, R. Duce, *Limnol. Oceanogr.* **36**, 1960 (1991).
6. J. H. Martin *et al.*, *Nature* **371**, 123 (1994).
7. The design of FeAXs has involved single or multiple infusion (time scale of days) of iron, as a salt dissolved in acidified seawater, and concurrent addition(s) of SF_6 to the surface mixed layer of initial areal extent (50 to 225 km^2). The use of the SF_6 conservative tracer was essential to track this mesoscale region of iron-enriched surface ocean and avoids the uncertainty imposed by fixed-point sampling in Eulerian studies. This design (in particular the amount of Fe added) has changed little between FeAXs because of the need to ensure a large measurable biogeochemical signal during a relatively short period in a logistically challenging and dynamic environment.
8. H. J. W. de Baar *et al.*, *J. Geophys. Res.* **110**, C09S16 (2005) and references therein.
9. FeNXs have examined naturally occurring blooms within HNLC waters near the Galapagos [see (*4*)], within the Antarctic Circumpolar Current (*8*), and recently near the Southern Ocean islands Crozet and Kerguelen, where the studies Crozex (Crozet Circulation, Iron Fertilization and Export Production Experiment) and KEOPS (Kerguelen: Etude Comparée de l'Océan et du Plateau en Surface et Subsurface) took place from November 2004 to January 2005 and during January and February 2005, respectively (*8*).
10. K. Banse, *Limnol. Oceanogr.* **36**, 1886 (1991).
11. G. B. Mitchell, E. A. Brody, O. Holm-Hansen, C. McClain, J. Bishop, *Limnol. Oceanogr.* **36**, 1662 (1991).
12. The model in (*11*) was based on an adaptation of Sverdrup's critical depth theory (i.e., the relationship between the respective depths of the mixed and euphotic zones) for Southern Ocean waters.
13. M. T. Maldonado *et al.*, *Limnol. Oceanogr.* **46**, 1802 (2001).
14. A. J. Watson, D. C. E. Bakker, A. J. Ridgewell, P. W. Boyd, C. S. Law, *Nature* **407**, 730 (2000).
15. D. A. Hutchins, K. W. Bruland, *Nature* **393**, 561 (1998).
16. W. O. Smith Jr., R. F. Anderson, J. K. Moore, L. A. Codispoti, J. M. Morrison, *Deep Sea Res. II* **47**, 3073 (2000).
17. P. W. Boyd *et al.*, *Limnol. Oceanogr.* **50**, 1872 (2005).
18. K. O. Buesseler *et al.*, *Deep Sea Res. II* **50**, 579 (2003).
19. F. M. M. Morel, J. G. Reuter, N. M. Price, *Oceanography* **4**, 56 (1990).
20. P. W. Boyd, S. Doney, in *Ocean Biogeochemistry—The Role of the Ocean Carbon Cycle in Global Change (JGOFS)*, M. J. R. Fasham, Ed. (Springer-Verlag, Berlin, 2003), pp. 157–187.
21. A. R. Bowie *et al.*, *Deep Sea Res. II* **47**, 1708 (2001).
22. M. L. Wells, *Mar. Chem.* **82**, 101 (2003).
23. P.W. Boyd, G. A. Jackson, A. M. Waite, *Geophys. Res. Lett.* **29**, 10.1029/2001GL014210 (2002).
24. Y. Le Clainche *et al.*, *J. Geophys. Res.* **111**, C01011 (2005).
25. T. D. Jickells *et al.*, *Science* **308**, 67 (2005).
26. K. Lochte, H. W. Ducklow, M. J. R. Fasham, C. Stienen, *Deep Sea Res. II* **40**, 91 (1993).
27. A. Abelmann, R. Gersonde, G. Cortese, G. Kuhn, V. Smetacek, *Paleoceanography* **21**, PA1013 (2006).
28. D. A. Hutchins, W. X. Wang, N. S. Fisher, *Limnol. Oceanogr.* **40**, 989 (1995).
29. B. W. Frost, *Nature* **383**, 475 (1996).
30. K. H. Coale, *Nature* **383**, 495 (1996).
31. A. R. Baker, T. D. Jickells, M. Witt, K. L. Linge, *Mar. Chem.* **98**, 43 (2006).
32. T. D. Jickells, *Mar. Chem.* **68**, 5 (1999).
33. B. A. Bergquist, E. A. Boyle, *Global Biogeochem. Cycles* **20**, GB1015 (2006).
34. J. Wu, E. Boyle, W. Sunda, L.-S. Wen, *Science* **292**, 847 (2001).
35. K. Johnson *et al.*, *Eos* **86** (Ocean Sci. Meet. Suppl.), abstract OS11N-02 (2006).
36. P. Parekh, M. J. Follows, E. A. Boyle, *Global Biogeochem. Cycles* **19**, GB2020 (2005).
37. J. K. B. Bishop, R. E. Davis, J. T. Sherman, *Science* **298**, 817 (2003).
38. K. S. Johnson *et al.*, *Global Biogeochem. Cycles* **17**, 10.1029/2002GB002004 (2003).
39. E. W. Wolff *et al.*, *Nature* **440**, 10.1038/nature04614 (2006).
40. N. Lefevre, A. J. Watson, *Global Biogeochem. Cycles* **13**, 727 (1999).
41. L. Bopp, K. E. Kohfeld, C. Le Quéré, O. Aumont, *Paleoceanography* **18**, 10.1029/2002PA000810 (2003).
42. R. D. Frew *et al.*, *Global Biogeochem. Cycles* **20**, 10.1029/2005GB002558 (2006).
43. W. G. Sunda, *Mar. Chem.* **57**, 169 (1997).
44. A. Gnanadesikan, J. L. Sarmiento, R. D. Slater, *Global Biogeochem. Cycles* **17**, 10.1029/2002GB001940 (2003).
45. R. Strzepek *et al.*, *Global Biogeochem. Cycles* **20**, 10.1029/2005GB002490 (2006).
46. L. J. Hoffmann, I. Peeken, K. Lochte, P. Assmy, M. Veldhuis, *Limnol. Oceanogr.* **51**, 1217 (2006).
47. J. Bell, J. Betts, E. Boyle, *Deep Sea Res. I* **49**, 2103 (2002).
48. H. E. Garcia, R. A. Locarnini, T. P. Boyer, J. I. Antonov, in *World Ocean Atlas 2005, vol. 4, Nutrients*, S. Levitus, Ed. (U.S. Government Printing Office, Washington, DC, 2006).
49. P. W. Boyd *et al.*, *Nature* **407**, 695 (2000).
50. B. S. Twining, S. B. Baines, N. S. Fisher, *Limnol. Oceanogr.* **49**, 2115 (2004).
51. J. H. Martin, S. E. Fitzwater, R. M. Gordon, C. N. Hunter, S. J. Tanner, *Deep Sea Res. II* **40**, 115 (1993).
52. P. W. Boyd *et al.*, *Deep Sea Res. II* **46**, 2761 (1999).
53. W. G. Sunda, S. A. Huntsman, *Mar. Chem.* **50**, 189 (1995).
54. K. O. Buesseler, J. E. Andrews, S. M. Pike, M. A. Charette, *Science* **304**, 414 (2004) doi:10.1126/science.1086895
55. P. Boyd, unpublished data from SERIES.
56. F. Gervais, U. Riebesell, M. Y. Gorbunov, *Limnol. Oceanogr.* **47**, 1324 (2002).
57. S. Takeda, A. Tsuda, *Prog. Oceanogr.* **64**, 95 (2004).
58. K. H. Coale *et al.*, *Science* **304**, 408 (2004).
59. SEEDS II took place in July 2004, SAGE in March–April 2004, and FeeP in May 2004. For more details, contact tsuda@ori.u-tokyo.ac.japan, m.harvey@niwa.co.nz, and njpo@pml.ac.uk, respectively.
60. The workshop "A Synthesis of Mesoscale Iron-Enrichments," held in Wellington in November 2005, was supported by the Surface Ocean–Lower Atmosphere Study, NSF, NIWA, the New Zealand Royal Society, the UK Royal Society, Belgian Federal Science Policy, and the Natural Sciences and Engineering Research Council of Canada. We thank E. McKay and K. Richardson for the graphics, and two anonymous reviewers for their helpful comments and insights. This manuscript is dedicated to the memory of R.B.